Space-Constrained Mixed-ADC Massive MIMO

Hessam Pirzadeh*, A. Lee Swindlehurst*, and Josef A. Nossek†
*Center for Pervasive Communications and Computing, University of California Irvine, Irvine, CA 92697, USA.
Email: {hpirzade, swindle}@uci.edu
†Department of Teleinformatics Engineering, Federal University of Ceara, Fortaleza 60020-181, Brazil.
Email: josef.a.nossek@tum.de

***Abstract*—The uplink performance of a mixed analog-to-digital converter (ADC) massive multiple-input multiple-output (MIMO) architecture with a space-constrained array at the base station (BS) is analyzed. We investigate the effect of spatial correlation and mutual coupling on the spectral efficiency (SE) of the system. First, we analyze to what extent adding a small number of high-resolution ADCs can impact the channel estimation accuracy. Then, we derive a closed-form approximation for the SE. Our analysis demonstrates how a space constraint on a uniform linear array (ULA) can affect the design of a massive MIMO system with low-resolution ADCs. It is shown that by equally spacing a small number of high-resolution ADCs over the array, one can dramatically reduce the performance gap between a system with all low-resolution and all high-resolution ADCs.**

I. Introduction

Power consumption is one of the main concerns for next generation wireless networks. Deploying power efficient base stations (BSs) while satisfying the high data rate demand is of crucial importance in designing next generation systems. Massive multiple-input multiple-output (MIMO) with low-resolution analog-to-digital converters (ADCs) is a viable approach to meet the aforementioned objectives.

The uplink performance of a massive MIMO system (in terms of spectral efficiency (SE)) with low-resolution ADCs was studied in [1] and [2] for independent Rayleigh fading and Rician channel models, respectively. It was shown that although exploiting low-resolution ADCs leads to SE loss, the main benefits of utilizing a large number of antennas at the BS is still achievable. In particular, it is shown that the performance loss due to using one-bit ADCs can be overcome by equipping the BS with more antennas [3]. However, the previous work assumed uncorrelated Rayleigh fading channels with no mutual coupling where adding more antennas at the BS does not impose any penalty on system performance [4], [5].

One of the challenges of deploying massive MIMO systems is to fit a large number of antennas in a constrained physical space [6]. In this scenario, adding more antennas leads to increasing spatial correlation and mutual coupling among adjacent antennas which can cause severe performance degradation. Hence, it is not possible to arbitrarily increase the number of antennas at the BS to offset the SE loss. In [7], it is observed that contrary to the Rayleigh fading case, the user's channels are no longer asymptotically orthogonal in the space-constrained scenario. The SE and energy efficiency of massive MIMO systems with space-constrained arrays are shown in [8], [9] to be concave functions of the number of antennas. This demonstrates that in space-constrained arrays, it is not beneficial to increase the number of antennas beyond a certain threshold within a limited physical space. In [10], the increased correlation among adjacent antennas in the space-constrained array is leveraged to reduce the RF chain complexity. The SE of a space-constrained array with linear receivers for Rayleigh and Rician fading channels is studied in [11] and [12], respectively.

Instead of equipping the BS with more antennas, an alternative approach to improve the performance of massive MIMO systems with low-resolution ADCs is to introduce a small fraction of high-resolution ADCs in the system for certain antennas [13]. The SE of such mixed-ADC architectures under Rayleigh and Rician fading channels is investigated in [14]-[16]. In [17], it is shown that, to obtain accurate channel state information in mixed-ADC architectures, round-robin training is required, which consumes a large portion of the available time-bandwidth resources. This makes mixed-ADC architecture with round-robin training unfavorable in channels with a short coherence interval.

In this work, we analyze the performance of mixed-ADC massive MIMO with space-constrained arrays. The Mixed-ADC architecture is a suitable approach to bridge the gap between massive MIMO with low- and high-resolution ADCs in space-constrained arrays. First, it does not require an increase in the number of antennas and therefore avoids the severe performance degradation due to mutual coupling. Moreover, it can take advantage of intrinsic correlation among adjacent antennas of a space-constrained array as done in [10]. This phenomenon can eliminate the need for round-robin training for channel estimation in mixed-ADC architectures. In this paper, we first analyze the channel estimation performance of such systems. Since the channel coefficients are correlated under the space-constrained assumption, high-resolution ADCs in a mixed-ADC architecture are added to improve the channel estimation accuracy of all channel coefficients. Based on this channel estimate, we exploit a maximum-ratio-combiner (MRC) at the BS and derive a closed-form approximation for the SE which explicitly shows the contribution of the low- and

This work was supported in part by the National Science Foundation under Grant ECCS-1547155 and Grant CCF-1703635 and in part by a Hans Fischer Senior Fellowship from the Technische Universität München Institute for Advanced Study. The work of J. A. Nossek has been performed in the framework of the Horizon 2020 project ONE5G (ICT-760809) receiving funds from the European Union.

978-1-5386-6528-2/19/$31.00 ©2019 IEEE

Authorized licensed use limited to: Access paid by The UC Irvine Libraries. Downloaded on May 19,2020 at 21:22:12 UTC from IEEE Xplore. Restrictions apply.

high-resolution ADCs on the SE of a mixed-ADC architecture with a space-constrained array. It is shown that by equally spacing the high-resolution ADCs over a uniform linear array, one can dramatically reduce the performance gap between a system with all low-resolution and all high-resolution ADCs.

Notation: We use boldface letters to denote vectors, and capitals to denote matrices. The (i,j) element of matrix $\mathbf{A}$ and the ith element of vector $\mathbf{a}$ are denoted by $[\mathbf{A}]_{ij}$ and a_i, respectively. The symbols $(.)^*$, $(.)^T$, $(.)^H$, and $\odot$ represent conjugate, transpose, conjugate transpose, and Hadamard product, respectively. A circularly-symmetric complex Gaussian (CSCG) random vector with zero mean and covariance matrix $\boldsymbol{R_v}$ is denoted by $\boldsymbol{v} \sim \mathcal{CN}(\mathbf{0}, \boldsymbol{R_v})$. We use $\mathrm{diag}\{\mathbf{C}\}$ to denote the diagonal matrix formed from the diagonal elements of the square matrix $\mathbf{C}$. $\boldsymbol{R_{uv}}$ denotes crosscorrelation of vectors $\boldsymbol{u}$ and $\boldsymbol{v}$. Ci(.), Si(.), $\mathbb{E}\{.\}$, $\mathcal{V}\{.\}$, and $\Re\{.\}$ denote cosine and sine integrals, the expectation and variance operator, and the real part of a complex value, respectively.

II. System Model

Consider the uplink of a single-cell multi-user MIMO system consisting of K single-antenna users that send their signals simultaneously to a BS equipped with a uniform linear array (ULA) with M antennas. The $M \times 1$ signal received at the BS from the K users is given by

$$\mathbf{y} = \sqrt{p}\mathbf{G}\mathbf{s} + \mathbf{n}, \tag{1}$$

where p represents the average transmission power from the users, $\mathbf{G} = [\mathbf{g}_1, \cdots, \mathbf{g}_K] \in \mathbb{C}^{M\times K}$ is the channel matrix between the users and the BS. The symbol vector transmitted by the users is denoted by $\mathbf{s} \in \mathbb{C}^{K\times 1}$ where $\mathbb{E}\left\{\mathbf{s}\mathbf{s}^H\right\} = \mathbf{I}_K$ and is drawn from a CSCG codebook independent of the other users, and, $\mathbf{n} \sim \mathcal{CN}(\mathbf{0}, \boldsymbol{R}_\mathbf{n})$ denotes additive CSCG receiver noise at the BS. The channel matrix can be decomposed as

$$\mathbf{G} = \mathbf{T}\mathbf{A}\mathbf{H}\mathbf{D}^{\frac{1}{2}}, \tag{2}$$

where $\mathbf{T}$ is the mutual coupling matrix which is defined as

$$\mathbf{T} = \left(\mathbf{I}_M + \frac{1}{R}\mathbf{Z}\right)^{-1} \tag{3}$$

where R denotes low noise amplifier (LNA) input impedance. For thin half wavelength dipoles, the elements of $\mathbf{Z}$ can be characterized as [19]

$$[\mathbf{Z}]_{ij} = 30\Big(2\mathrm{Ci}(2\pi d_{ij}) - \mathrm{Ci}(\xi_{ij}+\pi) - \mathrm{Ci}(\xi_{ij}-\pi) + j\left(-2\mathrm{Si}(2\pi d_{ij}) + \mathrm{Si}(\xi_{ij}+\pi) + \mathrm{Si}(\xi_{ij}-\pi)\right)\Big),\ i \neq j$$

$$[\mathbf{Z}]_{ii} = 30\big(\gamma + \log(2\pi) - \mathrm{Ci}(2\pi) + j\mathrm{Si}(2\pi)\big), \tag{4}$$

where d_{ij} is the distance between antennas i and j normalized by the wavelength, $\xi_{ij} = \pi\sqrt{1+4d_{ij}^2}$, and γ denotes the Euler-Mascheroni constant.

We consider a physical channel model where the angular domain is comprised of P finite directions, as in [18]. Hence, $\mathbf{A}$ is an $M \times P$ matrix whose pth column denotes the array steering vector corresponding to the direction of arrival $\varphi_p \in \left[-\frac{\pi}{2}, \frac{\pi}{2}\right]$ and is given by

$$\mathbf{a}(\varphi_p) = \frac{1}{\sqrt{P}}[1, e^{-j2\pi d_{12}\sin(\varphi_p)}, \cdots, e^{-j2\pi d_{1M}\sin(\varphi_p)}]^T, \tag{5}$$

and $\mathbf{H} = [\mathbf{h}_1, \cdots, \mathbf{h}_K] \in \mathbb{C}^{P\times K}$ is the propagation response matrix and represents the fast fading whose elements are distributed identically and independently as $\mathcal{CN}(0,1)$. Geometric attenuation and shadow fading are modeled by the diagonal matrix $\mathbf{D}$ whose kth diagonal element is denoted by β_k. In the remainder of the paper, we assume that $\mathbf{A}$ and $\mathbf{D}$ are priori known at the BS [11], [18]. By considering the mutual coupling effect, the additive noise covariance matrix, $\boldsymbol{R}_\mathbf{n}$, can be derived as

$$\boldsymbol{R}_\mathbf{n} = \mathbf{T}\big(\sigma_i^2(\mathbf{Z}\mathbf{Z}^H + R_N^2\mathbf{I}_M) - 2R_N\Re(\rho^*\mathbf{Z}) + 4\mathrm{k}TB\Re(\mathbf{Z})\big)\mathbf{T}^H, \tag{6}$$

with $\mathbb{E}\{\boldsymbol{i}_N\boldsymbol{i}_N^H\} = \sigma_i^2\mathbf{I}_M$, $\mathbb{E}\{\boldsymbol{u}_N\boldsymbol{u}_N^H\} = \sigma_u^2\mathbf{I}_M$, $R_N = \frac{\sigma_u}{\sigma_i}$, $\mathbb{E}\{\boldsymbol{u}_N\boldsymbol{i}_N^H\} = \frac{\rho}{\sigma_u\sigma_i}\mathbf{I}_M$, where $\boldsymbol{i}_N$ and $\boldsymbol{u}_N$ denote the equivalent noise current and voltage of the LNA and k, T, and B represent the Boltzman constant, environment temperature, and bandwidth, respectively.

We consider a mixed-ADC architecture at the BS in which M_0 antennas are connected to high-resolution ADCs while M_1 antennas are fed to low-resolution ADCs. As a result, by partitioning the channel matrix $\mathbf{G}$, we can rewrite (1) as

$$\begin{bmatrix}\mathbf{y}_0\\ \mathbf{y}_1\end{bmatrix} = \sqrt{p}\begin{bmatrix}\mathbf{G}_0\\ \mathbf{G}_1\end{bmatrix}\mathbf{s} + \begin{bmatrix}\mathbf{n}_0\\ \mathbf{n}_1\end{bmatrix}. \tag{7}$$

In (7), $\mathbf{G}_0 = \mathbf{T}_0\mathbf{A}\mathbf{H}\mathbf{D}^{\frac{1}{2}} \in \mathbb{C}^{M_0\times K}$ ($\mathbf{G}_1 = \mathbf{T}_1\mathbf{A}\mathbf{H}\mathbf{D}^{\frac{1}{2}} \in \mathbb{C}^{M_1\times K}$) contains the channel coefficients from the users to the M_0 (M_1) antennas connected to high-resolution (low-resolution) ADCs and $\mathbf{n}_0$ ($\mathbf{n}_1$) denotes the corresponding elements of $\mathbf{n}$, and similarly for $\mathbf{T}_0$ and $\mathbf{T}_1$. Therefore, the received signal at the BS is

$$\mathbf{r} = \begin{bmatrix}\mathbf{r}_0\\ \mathbf{r}_1\end{bmatrix} = \begin{bmatrix}\mathbf{y}_0\\ \mathcal{Q}(\mathbf{y}_1)\end{bmatrix}, \tag{8}$$

where $\mathcal{Q}(\cdot)$ represents the element-wise quantization operation. We adopt the additive quantization noise model (AQNM) for the quantizer output [1]-[15]

$$\mathcal{Q}(\mathbf{y}_1) = \alpha\mathbf{y}_1 + \mathbf{q}, \tag{9}$$

where $0 < \alpha < 1$ is a linear gain dependent on the number of quantization bits and $\mathbf{q}$ denotes the quantization noise which is uncorrelated with $\mathbf{y}_1$ and whose covariance matrix is given by

$$\mathbf{R}_\mathbf{q} = \alpha(1-\alpha)\,\mathrm{diag}(\mathbf{R}_{\mathbf{y}_1}), \tag{10}$$

where $\mathbf{R}_{\mathbf{y}_1}$ denotes the covariance of $\mathbf{y}_1$.

Authorized licensed use limited to: Access paid by The UC Irvine Libraries. Downloaded on May 19,2020 at 21:22:12 UTC from IEEE Xplore. Restrictions apply.

We assume a block-fading model where each channel remains constant in a coherence interval of length T symbols and changes independently between different intervals. At the beginning of each coherence interval, the users send their η-tuple mutually orthogonal pilot sequences ($K \leq \eta \leq T$) to the BS for channel estimation. The remaining $T-\eta$ symbols are dedicated to uplink data transmission.

III. Training Phase

In this section, we investigate the linear minimum mean squared error (LMMSE) channel estimator for different ADC architectures at the BS. In all scenarios, the pilot sequences are drawn from an $\eta \times K$ matrix $\mathbf{\Phi}$, where the kth column of $\mathbf{\Phi}$, $\boldsymbol{\phi}_k$, is the kth user's pilot sequence and $\mathbf{\Phi}^H\mathbf{\Phi} = \boldsymbol{I}_K$. Therefore, the $M \times \eta$ received signal at the BS becomes

$$\mathbf{Y} = \begin{bmatrix}\mathbf{Y}_0\\ \mathbf{Y}_1\end{bmatrix} = \sqrt{\eta p}\begin{bmatrix}\mathbf{G}_0\\ \alpha\mathbf{G}_1\end{bmatrix}\mathbf{\Phi}^{\boldsymbol{T}} + \begin{bmatrix}\mathbf{N}_0\\ \alpha\mathbf{N}_1 + \mathbf{N}_q\end{bmatrix}, \tag{11}$$

where $\mathbf{N}_0$ ($\mathbf{N}_1$) is an $M_0 \times \eta$ ($M_1 \times \eta$) additive noise matrix and $\mathbf{N}_q$ denotes the quantization noise. The LMMSE estimate of the k-th user propagation response, $\mathbf{h}_k$, is

$$\hat{\mathbf{h}}_k = \sqrt{\eta p \beta_k}\mathbf{B}^H\left(\eta p \beta_k \mathbf{B}\mathbf{B}^H + \mathbf{R}_{\mathbf{w}}\right)^{-1}\mathbf{Y}\phi_k^*, \tag{12}$$

where

$$\mathbf{B} = \begin{bmatrix}\mathbf{T}_0\mathbf{A}\\ \alpha\mathbf{T}_1\mathbf{A}\end{bmatrix},\ \mathbf{R}_{\mathbf{w}} = \begin{bmatrix}\mathbf{R}_{\mathbf{n}_0} & \alpha\mathbf{R}_{\mathbf{n}_0\mathbf{n}_1}\\ \alpha\mathbf{R}_{\mathbf{n}_1\mathbf{n}_0} & (\alpha^2\mathbf{R}_{\mathbf{n}_1} + \mathbf{R}_{\mathbf{q}})\end{bmatrix} \tag{13}$$

$$\mathbf{R}_{\mathbf{q}} = \alpha(1-\alpha)\mathrm{diag}\left(p\left(\sum_{k=1}^{K}\beta_k\right)\mathbf{T}_1\mathbf{A}\mathbf{A}^H\mathbf{T}_1^H + \mathbf{R}_{\mathbf{n}_1}\right). \tag{14}$$

By defining the channel estimation error, $\boldsymbol{\epsilon} = \mathbf{h}_k - \hat{\mathbf{h}}$, we have

$$\mathbf{R}_{\hat{\mathbf{h}}_k} = \eta p \beta_k \mathbf{B}^H\left(\eta p \beta_k \mathbf{B}\mathbf{B}^H + \mathbf{R}_{\mathbf{w}}\right)^{-1}\mathbf{B} \tag{15}$$

$$\mathbf{R}_{\boldsymbol{\epsilon}_k} = \left(\mathbf{I}_P + \eta p \beta_k \mathbf{B}^H\mathbf{R}_{\mathbf{w}}^{-1}\mathbf{B}\right)^{-1} \tag{16}$$

where $\mathbf{R}_{\hat{\mathbf{h}}_k}$ and $\mathbf{R}_{\boldsymbol{\epsilon}_k}$ denote the covariance matrix of $\hat{\mathbf{h}}_k$ and $\boldsymbol{\epsilon}$, respectively.

In contrast with independent Rayleigh fading channel where each high-resolution ADC only can improve the estimation accuracy of the channel associated with the antenna connected to it [14], in this model each high-resolution observation sees information about all P channel coefficients coefficients due to the coupling matrix $\mathbf{T}$ and array steering matrix $\mathbf{A}$. Hence, the high-resolution ADCs will have a stronger contribution to increasing the estimation accuracy of all channel coefficients due to the correlation among the observations. In Section V, we numerically show to what extent adding a small number of high-resolution ADCs improves the channel estimation accuracy.

IV. Spectral Efficiency

In the data transmission phase, all users simultaneously send their data symbols to the BS. Without loss of generality, we index the antennas such that the first N are connected to high-resolution ADCs. From equation (1), the received signal at the BS after quantization can be approximated as [15]:

$$\begin{bmatrix}\mathbf{r}_0\\ \mathbf{r}_1\end{bmatrix} \approx \begin{bmatrix}\sqrt{p}\mathbf{G}_0\mathbf{s} + \mathbf{n}_0\\ \sqrt{p}\alpha\mathbf{G}_1\mathbf{s} + \alpha\mathbf{n}_1 + \mathbf{q}_d\end{bmatrix}, \tag{17}$$

where $\mathbf{q}_d$ denotes the quantization noise whose covariance matrix is given by:

$$\mathbf{R}_{\mathbf{q}_d} = \alpha\left(1-\alpha\right)\mathrm{diag}\left(p\mathbf{G}_1\mathbf{G}_1^H + \mathbf{R}_{n_1}\right). \tag{18}$$

For data detection, the BS uses the MRC receiver $\boldsymbol{W} = \hat{\mathbf{G}}$ where $\hat{\mathbf{G}} = [\hat{\mathbf{g}}_1, ..., \hat{\mathbf{g}}_K]$ denotes the estimate of the channel. Therefore, the resulting signal at the BS is

$$\hat{\mathbf{s}} = \mathbf{W}^H\begin{bmatrix}\mathbf{r}_0\\ \mathbf{r}_1\end{bmatrix} = \sqrt{p}\begin{bmatrix}\hat{\mathbf{G}}_0\\ \hat{\mathbf{G}}_1\end{bmatrix}^H\begin{bmatrix}\mathbf{G}_0\\ \alpha\mathbf{G}_1\end{bmatrix}\mathbf{s} + \begin{bmatrix}\hat{\mathbf{G}}_0\\ \hat{\mathbf{G}}_1\end{bmatrix}^H\begin{bmatrix}\mathbf{n}_0\\ \alpha\mathbf{n}_1 + \mathbf{q}_d\end{bmatrix}. \tag{19}$$

The kth element of $\hat{\mathbf{s}}$ is

$$\begin{aligned}\hat{s}_k = \sqrt{p}\left(\hat{\mathbf{g}}_{0k}^H\hat{\mathbf{g}}_{0k} + \alpha\hat{\mathbf{g}}_{1k}^H\hat{\mathbf{g}}_{1k}\right)s_k + \\ \sqrt{p}\sum_{i=1,i\neq k}^{K}\left(\hat{\mathbf{g}}_{0k}^H\hat{\mathbf{g}}_{0i} + \alpha\hat{\mathbf{g}}_{1k}^H\hat{\mathbf{g}}_{1i}\right)s_i + \\ \sqrt{p}\sum_{i=1}^{K}\left(\hat{\mathbf{g}}_{0k}^H\varepsilon_{0i} + \alpha\hat{\mathbf{g}}_{1k}^H\varepsilon_{1i}\right)s_i + \\ \hat{\mathbf{g}}_{0k}^H\mathbf{n}_0 + \alpha\hat{\mathbf{g}}_{1k}^H\mathbf{n}_1 + \hat{\mathbf{g}}_{1k}^H\mathbf{q}_d,\end{aligned} \tag{20}$$

where $\hat{\mathbf{g}}_{0k}$, $\hat{\mathbf{g}}_{1k}$, $\varepsilon_{0k} \triangleq \mathbf{g}_{0k} - \hat{\mathbf{g}}_{0k}$, $\varepsilon_{1k} \triangleq \mathbf{g}_{1k} - \hat{\mathbf{g}}_{1k}$ are the kth columns of $\hat{\mathbf{G}}_0$, $\hat{\mathbf{G}}_1$, $\mathcal{E}_0 \triangleq \mathbf{G}_0 - \hat{\mathbf{G}}_0$, and $\mathcal{E}_1 \triangleq \mathbf{G}_1 - \hat{\mathbf{G}}_1$, respectively. The BS treats $\hat{\mathbf{g}}_{0k}^H\hat{\mathbf{g}}_{0k} + \alpha\hat{\mathbf{g}}_{1k}^H\hat{\mathbf{g}}_{1k}$ as the desired channel and the other terms of (20) as Gaussian noise when decoding the signal. Consequently, a lower bound for the ergodic achievable SE at the kth user can be written as [15]

$$\mathcal{S}_k = \left(1 - \frac{\eta}{T}\right)\mathbb{E}\left\{\log_2\left(1 + \frac{p \mid \hat{\mathbf{g}}_{0k}^H\hat{\mathbf{g}}_{0k} + \alpha\hat{\mathbf{g}}_{1k}^H\hat{\mathbf{g}}_{1k} \mid^2}{\Omega}\right)\right\}, \tag{21}$$

where

$$\begin{aligned}\Omega = p\sum_{i=1,i\neq k}^{K}|\hat{\mathbf{g}}_{0k}^H\hat{\mathbf{g}}_{0i} + \alpha\hat{\mathbf{g}}_{1k}^H\hat{\mathbf{g}}_{1i}|^2 + \\ p\sum_{i=1}^{K}\beta_i\Big(\hat{\mathbf{g}}_{0k}^H\mathbf{A}_0\mathbf{R}_{\boldsymbol{\epsilon}_i}\mathbf{A}_0^H\hat{\mathbf{g}}_{0k}^H + \alpha^2\hat{\mathbf{g}}_{1k}^H\mathbf{A}_1\mathbf{R}_{\boldsymbol{\epsilon}_i}\mathbf{A}_1^H\hat{\mathbf{g}}_{1k}^H + \\ 2\alpha\Re\left\{\hat{\mathbf{g}}_{0k}^H\mathbf{A}_0\mathbf{R}_{\boldsymbol{\epsilon}_i}\mathbf{A}_1^H\hat{\mathbf{g}}_{1k}^H\right\}\Big) + \\ \sigma_n^2\left(\|\hat{\mathbf{g}}_{0k}\|^2 + \alpha^2\|\hat{\mathbf{g}}_{1k}\|^2\right) + \\ \alpha\left(1-\alpha\right)\hat{\mathbf{g}}_{1k}^H\mathrm{diag}\left(p\left(\hat{\mathbf{G}}_1 - \mathcal{E}_1\right)\left(\hat{\mathbf{G}}_1 - \mathcal{E}_1\right)^H + \mathbf{R}_{\mathbf{n}_1}\right)\hat{\mathbf{g}}_{1k}\end{aligned} \tag{22}$$

with $\mathbf{A}_t \triangleq \mathbf{T}_t\mathbf{A}$.

Authorized licensed use limited to: Access paid by The UC Irvine Libraries. Downloaded on May 19,2020 at 21:22:12 UTC from IEEE Xplore. Restrictions apply.

An approximation for the achievable SE of a mixed-ADC system with mutual coupling and MRC detection is presented in the next theorem.

***Theorem* 1.** *For a mixed-ADC massive MIMO system with MRC detection and an array of thin dipoles, the SE of the kth user is*

$$\mathcal{S}_k \approx \left(1-\frac{\eta}{T}\right)\log_2\left(1+\frac{\mathcal{A}}{\mathcal{I}+\mathcal{B}+\mathcal{N}+\alpha(1-\alpha)\mathcal{Q}}\right), \tag{23}$$

when mutual coupling effects are considered, where $\mathcal{A}$, $\mathcal{I}$, $\mathcal{B}$, $\mathcal{N}$, and $\mathcal{Q}$ are shown at the top of the next page, and

$$\Gamma_{tk}=\mathbf{R}_{\hat{\mathbf{h}}_k}\mathbf{A}_t^H\mathbf{A}_t,\ t\in\{0,1\},\ \Gamma_{tk}^{\epsilon}=\mathbf{R}_{\epsilon_k}\mathbf{A}_t^H\mathbf{A}_t,\ t\in\{0,1\}$$

$$\tilde{\Gamma}_{tk}=\mathbf{A}_t\mathbf{R}_{\hat{\mathbf{h}}_k}\mathbf{A}_t^H,\ t\in\{0,1\},\ \tilde{\Gamma}_{tk}^{\epsilon}=\mathbf{A}_t\mathbf{R}_{\epsilon_k}\mathbf{A}_t^H,\ t\in\{0,1\}.$$

Proof. From [15], [20], an approximation for (21) can be calculated as

$$\mathcal{S}_k=\left(1-\frac{\eta}{T}\right)\log_2\left(1+\frac{p\mathbb{E}\left\{|\ \hat{\mathbf{g}}_{0k}^H\hat{\mathbf{g}}_{0k}+\alpha\hat{\mathbf{g}}_{1k}^H\hat{\mathbf{g}}_{1k}\ |^2\right\}}{\mathbb{E}\left\{\Omega\right\}}\right). \tag{29}$$

Using Lemma 2 of [21], the expected values of the desired signal, interference, and noise can be easily calculated. To calculate the expected value of the last term in (22), we have

$$\mathbb{E}\left\{\hat{\mathbf{g}}_{1k}^H\mathrm{diag}\left(p\left(\hat{\mathbf{G}}_1-\mathcal{E}_1\right)\left(\hat{\mathbf{G}}_1-\mathcal{E}_1\right)^H+\mathbf{R}_{n1}\right)\hat{\mathbf{g}}_{1k}\right\}$$

$$=p\sum_{m=1}^{M_1}\sum_{i\neq k}^{K}\mathbb{E}\left\{|\hat{g}_{1km}|^2\right\}\mathbb{E}\left\{|g_{1im}|^2\right\}+$$
$$p\sum_{m=1}^{M_1}\mathbb{E}\left\{|\hat{g}_{1km}|^4\right\}+\mathbb{E}\left\{|\hat{g}_{1km}|^2|\varepsilon_{1km}|^2\right\}+$$
$$\mathbb{E}\left\{\hat{\mathbf{g}}_{1k}^H\mathbf{R}_{\mathbf{n}_1}\hat{\mathbf{g}}_{1k}\right\}.$$

Given that $\mathbb{E}\left\{|g_{1im}|^2\right\}=\beta_i\left[\mathbf{A}_1\mathbf{A}_1^H\right]_{mm}$, we need to calculate the expected values of $\sum_{m=1}^{M}|\hat{g}_{1km}|^2$, $\sum_{m=1}^{M}|\hat{g}_{1km}|^4$, and $\sum_{m=1}^{M}|\hat{g}_{1km}|^2|\varepsilon_{1km}|^2$. Since $\hat{g}_{1km}$ is a complex normal random variable with variance $\mathbb{E}\left\{|\hat{g}_{1km}|^2\right\}=\beta_k\left[\tilde{\Gamma}_{1k}\right]_{mm}$, we have $\mathbb{E}\left\{|\hat{g}_{1km}|^4\right\}=2\beta_k^2\left[\tilde{\Gamma}_{1k}\right]_{mm}^2$. Hence

$$\sum_{m=1}^{M_1}\mathbb{E}\left\{|\hat{g}_{1km}|^4\right\}=2\beta_k^2\mathrm{Tr}(\tilde{\Gamma}_{1k}\odot\tilde{\Gamma}_{1k}). \tag{30}$$

The expected value of $\sum_{m=1}^{M}|\hat{g}_{1km}|^2|\varepsilon_{1km}|^2$ can be derived similarly. ∎

In the next section, we show how adding a small number of high-resolution ADCs impacts the channel estimation accuracy and SE of the system.

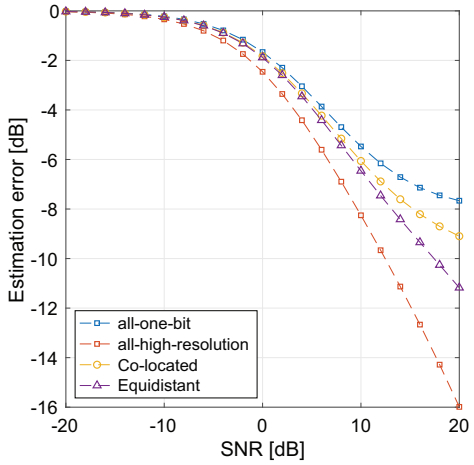

Fig. 1. Channel estimation error versus SNR.

V. Numerical Results

In this section, we numerically investigate the performance of the space-constrained mixed-ADC massive MIMO system in terms of channel estimation error and SE. We assume static-aware power control in the network [22], so that $p=p_0/\beta_k$. Furthermore, we assume $K=\eta=10$, and a uniform linear array with uniformly distributed angle of arrivals, i.e., $\varphi_p=-\pi/3+(p-1)\pi/P,\ p=1,\ \ldots,\ P$ as in [18]. The normalized distance between antenna elements is denoted by $d=d_{\mathrm{ap}}/M$ where d_{ap} is the normalized array length. In all figures, we assume $T=200$, $P=20$, and $\mathrm{SNR}\triangleq\frac{p_0}{\mathbf{R}_{\mathbf{n}}(1,1)}$.

Fig. 1 shows the advantage of the mixed-ADC architecture in the channel estimation phase for a system with $M=100$ antennas and $d_{\mathrm{ap}}=10$. As a benchmark, we have sketched the channel estimation error, i.e., $\frac{1}{P}\mathrm{Tr}\left(\mathbf{R}_{\epsilon}\right)$, of a system with all 1-bit ADCs and all-high-resolution ADCs. "Co-located" denotes a mixed-ADC system with $M_0=20$ high-resolution ADCs which are embedded in the array side by side. "Equidistant" refers to a mixed-ADC system where the high-resolution ADCs are equally spaced over the array. It can be seen that the mixed-ADC architecture with equidistant spacing reduces the gap between the all-high-resolution architecture and the all-1-bit architecture by one half at high SNRs.

As mentioned above, one approach to compensate for SE loss when all antennas are connected to low-resolution ADCs is to increase the number of antennas. However, this is true only for the case that there is no constraint on the size of the array. As we show in the next example, when the array size is constrained, increasing the number of antennas can lead to saturation in SE. Therefore, the only viable approach to achieve a predefined SE seems to be through a mixed-ADC architecture.

Fig. 2 shows the impact of increasing the number of antennas for different array lengths d_{ap}. It can be seen that as long as the antenna spacing is greater than half a wavelength, the SE increases monotonically as a function of the number of antennas at the BS. Eventually, the SE of the system saturates

Authorized licensed use limited to: Access paid by The UC Irvine Libraries. Downloaded on May 19,2020 at 21:22:12 UTC from IEEE Xplore. Restrictions apply.

$$\mathcal{A} = p\beta_k \left(|\mathrm{Tr}(\Gamma_{0k})|^2 + \mathrm{Tr}(\Gamma_{0k}^2) + \alpha^2 \left(|\mathrm{Tr}(\Gamma_{1k})|^2 + \mathrm{Tr}(\Gamma_{1k}^2) \right) + 2\alpha \Re \left\{ \mathrm{Tr}(\Gamma_{0k}\Gamma_{1k})\mathrm{Tr}(\Gamma_{0k})\mathrm{Tr}(\Gamma_{1k}) \right\} \right) \tag{24}$$

$$\mathcal{I} = p \sum_{i \neq k}^{K} \beta_i (\mathrm{Tr}\left(\Gamma_{0k}\Gamma_{0i}\right) + \alpha^2 \mathrm{Tr}(\Gamma_{1k}\Gamma_{1i}) + 2\alpha \Re \left\{ \mathrm{Tr}(\Gamma_{0k}\Gamma_{1i}) \right\}) \tag{25}$$

$$\mathcal{B} = p \sum_{i = k}^{K} \beta_i (\mathrm{Tr}\left(\Gamma_{0k}\Gamma_{0i}^{\epsilon}\right) + \alpha^2 \mathrm{Tr}(\Gamma_{1k}\Gamma_{1i}^{\epsilon}) + 2\alpha \Re \left\{ \mathrm{Tr}(\Gamma_{0k}\Gamma_{1i}^{\epsilon}) \right\}) \tag{26}$$

$$\mathcal{N} = \mathrm{Tr}\left(\mathbf{R}_{\hat{\mathbf{h}}_k} (\mathbf{TA})^H \begin{bmatrix} \mathbf{R}_{\mathbf{n}_0} & \alpha \mathbf{R}_{\mathbf{n}_0\mathbf{n}_1} \\ \alpha \mathbf{R}_{\mathbf{n}_1\mathbf{n}_0} & \alpha^2 \mathbf{R}_{\mathbf{n}_1} \end{bmatrix} \mathbf{TA} \right) \tag{27}$$

$$\mathcal{Q} = p \left(\sum_{i \neq k}^{K} \beta_i \right) \mathrm{Tr}(\tilde{\Gamma}_{1k} \odot (\mathbf{A}_1 \mathbf{A}_1^H)) + 2p\beta_k \mathrm{Tr}(\tilde{\Gamma}_{1k} \odot \tilde{\Gamma}_{1k}) + p\beta_k \mathrm{Tr}(\tilde{\Gamma}_{1k} \odot \tilde{\Gamma}_{1k}^{\epsilon}) + \mathrm{Tr}\left(\mathbf{R}_{\hat{\mathbf{h}}_k} (\mathbf{T_1 A})^H \mathbf{R}_{\mathbf{n}_1} \mathbf{T_1 A} \right) \tag{28}$$

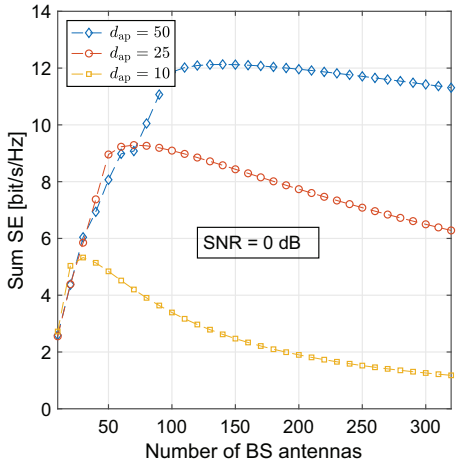

Fig. 2. Sum SE versus the number of BS antennas, M, for $\mathrm{SNR} = 0$ dB, and different d_{ap}. 20% of the antennas are connected to high-resolution ADCs.

and is maximized at a certain number of antennas.

REFERENCES

[1] L. Fan, S. Jin, C. Wen, and V. Zhang, "Uplink achievable rate for massive MIMO systems with low-resolution ADC," *IEEE Commun. Lett.*, vol. 19, no. 12, pp. 2186-2189, Dec. 2015.

[2] J. Zhang, L. Dai, S. Sun, and Z. Wang, "On the spectral efficiency of massive MIMO systems with low-resolution ADCs," *IEEE Commun. Lett.*, vol. 20, no. 5, pp. 842-845, May. 2016.

[3] Y. Li, C. Tao, L. Liu, A. Mezghani, G. Seco-Granados, and A. Swindlehurst, "Channel estimation and performance analysis of one-bit massive MIMO systems," *IEEE Trans. Signal Process.*, vol. 65, no. 15, pp. 4075-4089, May 2017.

[4] H. Pirzadeh, and A. L. Swindlehurst, "Spectral efficiency under energy constraint for mixed-ADC MRC massive MIMO," *IEEE Sig. Process. Lett.*, vol. 24, no. 12, pp. 1847-1851, Oct. 2017.

[5] K. Senel, E. Björnson, and E. G. Larsson, "Optimal base station design with limited fronthaul: Massive bandwidth or massive MIMO?," *Arxiv preprint*, arXiv:1709.05172.

[6] C. Masorous, M. Sellathurai, and T. Ratnarajah, "Large-Scale MIMO transmitters in fixed physical spaces: The effect of transmit correlation and mutual coupling," *IEEE Trans. Commun.*, vol. 61, no. 7, pp. 2794-2804, July 2013.

[7] C. Masorous, and M. Matthaiou, "Space-constrained massive MIMO: Hitting the wall of favorable propagation," *IEEE Commun. Lett.*, vol. 19, no. 5, pp. 771-774, May 2015.

[8] S. Biswas, C. Masorous, and T. Ratnarajah, "Performance analysis of large multiuser MIMO systems with space-constrained 2-D antenna arrays," *IEEE Trans. Wireless Commun.*, vol. 15, no. 5, pp. 3492-3505, May 2016.

[9] X. Ge, R. Zi, H. Wang, J. Zhang, and M. Jo, "Multi-User massive MIMO communication systems based on irregular antenna arrays," *IEEE Trans. Wireless Commun.*, vol. 15, no. 8, pp. 5287-5301, Aug. 2016.

[10] A. Garcia-Rodriguez, and C. Masorous, "Exploiting the increasing correlation of space constrained massive MIMO for CSI relaxation," *IEEE Trans. Commun.*, vol. 64, no. 4, pp. 1572-1587, April 2016.

[11] J. Zhang, L. Dai, M. Matthaiou, C. Mosorous, and S. Jin, "On the spectral efficiency of space-constrained massive MIMO with linear receivers," in *Proc. IEEE Int. Conf. on Commun. (ICC), 2016.*

[12] H. Tataria, P. J. Smith, M. Matthaiou, and P. A. Dmochowski, "Uplink analysis of large MU-MIMO systems with space-constrained arrays in ricean fading," in *Proc. IEEE Int. Conf. on Commun. (ICC), 2017.*

[13] N. Liang, W. Zhang, "Mixed-ADC massive MIMO," *IEEE J. Sel. Areas in Commun.*, vol. 34, no. 4, pp. 983-997, April 2016.

[14] W. Tan, S. Jin, C. Wen and Y. Jing, "Spectral efficiency of mixed-ADC receivers for massive MIMO systems," *IEEE Access*, vol. 4, pp. 7841-7846, Aug. 2016.

[15] J. Zhang, L. Dai, Z. He, S. Jin, and X. Li, "Performance analysis of mixed-ADC massive MIMO systems over Rician fading channels," *IEEE J. Sel. Areas in Commun.*, vol. 35, no. 6, pp. 1327-1338, June 2017.

[16] J. Park, S. Park, A. Yazdan and R. W. Heath "Optimization of Mixed-ADC multi-antenna systems for Cloud-RAN deployments," *IEEE Trans. Commun.*, vol. 65, no. 9, pp. 3962-3975, Sep. 2017.

[17] H. Pirzadeh, and A. L. Swindlehurst, "Spectral efficiency of Mixed-ADC massive MIMO," *IEEE Trans. Sig. Process.*, vol. 66, no. 13, pp. 3599-3613, July 2018.

[18] H. Q. Ngo, E. G. Larsson, and T. L. Marzetta, "The multicell multiuser MIMO uplink with very large antenna arrays and a finite-dimensional channel," *IEEE Trans. Commun.*, vol. 61, no. 6, pp. 2350-2361, June 2013.

[19] S. A. Schelkunoff, *Antennas: Theory and Practice*. New York: John Wiley and Sons, 1952.

[20] Q. Zhang, S. Jin, K-K. Wang, H. Zhu, and M. Matthaiou "Power scaling of uplink massive MIMO systems with arbitrary-rank channel means," *IEEE Journal of Sel. Topics Sig. Process.*, vol. 8, no. 5, pp. 966-981, Oct. 2014.

[21] E. Björnson, M. Matthaiou, and M. Debbah, "Massive MIMO with non-ideal arbitrary arrays: Hardware scaling laws and circuit-aware design," *IEEE Trans. Wireless Commun.*, vol. 14, no. 8, pp. 4353-4368, Aug. 2015.

[22] E. Björnson, E. G. Larsson, and M. Debbah, "Massive MIMO for maximal spectral efficiency: How many users and pilots should be allocated?," *IEEE Trans. Wireless Commun.*, vol. 15, no. 2, pp. 1293-1308, Feb. 2016.

Authorized licensed use limited to: Access paid by The UC Irvine Libraries. Downloaded on May 19,2020 at 21:22:12 UTC from IEEE Xplore. Restrictions apply.